Experimental Study on the Curing Mechanism of Red Mud-Based Stabilized Soil Co-Modified by Nano-SiO2 and Gypsum

Chen Shengjin * , Ou Xiaoduo , Jiang Jie , Tan Zhijie

Posted Date: 12 July 2023

doi: 10.20944/preprints202307.0853.v1

Keywords: red mud; nano-SiO2; synergistic modification; stabilized soil; curing mechanism

Article

Experimental Study on the Curing Mechanism of Red Mud-Based Stabilized Soil Co-Modified by Nano-SiO_2 and Gypsum

Chen Shengjin [1], Ou Xiaoduo [2,*], Jiang Jie [2] and Tan Zhijie [1]

[1] Guangxi Hualan Geotechnical Engineering Co., Ltd, Nanning, Guangxi 530016; 278742250@qq.com (C.S.); 635166029@qq.com (T.Z.)
[2] Guangxi University, Nanning, Guangxi 530004; 51654964@qq.com
* Correspondence: ouxiaoduo@163.com

Abstract: In order to effectively utilize red mud and reduce its occupation of land resources as well as its impact on the environment, experiments were conducted to develop stabilized soil materials using nano-SiO_2 synergistically modified red mud and to investigate the curing mechanism of stabilized soil. The unconfined compressive strength, microscopic morphology and curing mechanism of the red mud-based stabilized soil materials with different amounts of modified materials were investigated. The test results show that after 7-days curing, the unconfined compressive strength of red mud-based stabilized soil meets the compressive strength requirement of road base material when nano-SiO_2, gypsum and cement are synergistically modified. In such case, the soil structure has the lowest fracture rate and the best structural compactness when the amount of nano-SiO2 is 1%; It is found that the needle-like and columnar calcium alumina in the modified red mud-based stabilized soil increases, and the binding energy of hydration product ions in the modified material is improved; The chemical curing mechanism of modified red mud-based stabilized soil includes hydration reaction, volcanic ash reaction, promotion effect of nano-SiO2, and enhancement effect of gypsum. On this base, a model of early start hydration process of red mud-based stabilized soil promoted by nano-SiO_2 is established.

Keywords: red mud; nano-SiO_2; synergistic modification; stabilized soil; curing mechanism

1. Introduction

Red mud, which is of high iron oxide content and red color, is a solid waste generated during the process of alkali alumina production. According to relevant statistics, for every 1 ton of alumina produced, 1 to 2 tons of red mud is generated (Wang et al., 2019; Zhu et al., 2016a). Currently, red mud is disposed of by open damming and stockpiling. The utilization of red mud is strictly controlled (Bombik et al., 2020; Xue et al., 2016a), making the utilization rate of red mud extremely low (less than 10% utilized so far, Xie et al., 2020; Mukiza et al., 2019), and red mud has become one of the bulk industrial solid wastes . Therefore, it is of practical significance to change the treatment of red mud from simple stockpiling to resource-based integrated utilization.

Red mud can be used to make ceramics and bricks, used as raw material for cement production, applied to road base materials, etc. By considering that road base materials can consume large amounts of red mud (Liang et al., 2021; Liu et al., 2018), currently, the research on the application of red mud in engineering is hot and has shown great potential (Ou et al., 2022; Suo et al., 2021; Atan et al., 2021). Mukiza et al., (2019) investigated the possibility of using red mud as a road base material, showing that the synergistic use of red mud and other wastes can improved the mechanical properties and durability performance of the material compared to red mud alone. Zhang et al., (2018) conducted experiments to determine the optimal ratio of red mud-based blends as road base materials, and proved that they can be used in road base through freeze-thaw tests, dry shrinkage tests, temperature shrinkage tests, and erosion resistance Li et al., (2020) studied the effect of gypsum on red mud-slag roadbed grouting material and found that gypsum can reduce the fluidity of red

Preprints (www.preprints.org) | NOT PEER-REVIEWED | Posted: 12 July 2023 doi:10.20944/preprints202307.0853.v1

mud-slag grouting material and can improve the compressive strength of grouting material. Zhang et al., (2019) prepared road base material using electrolytic manganese slag-red mud-electrolytic slag as the main raw material, and the results showed that the road base material hydrated to produce C-A-S-H gel and calcium alumina, and the road base material had high unconfined compressive strength strength and good durability. Li et al., (2022) studied the effect of calcium bentonite on the working performance of red mud-based grouting material, and further demonstrated that the road base material had high strength and durability because the red mud-based grouting material has a dense pore structure and high material strength. Through the above literature, it can be seen that scholars have conducted in-depth research on the feasibility of the red mud road base material and also analyzed its causal mechanism in depth.

Nanomaterials are extremely small particles with a particle size of 1 to 100 nm, with high specific surface area and good volcanic ash activity (Li et al., 2020). Scholars have introduced nano-SiO_2 materials into the field of civil engineering, and their main applications are improvement of concrete materials and soils (Kulkarni et al., 2022; Farajzadehha et al., 2021; Almurshedi et al., 2020; Adamu et al., 2018). The performance advantages of nano-SiO_2 are obvious, but how to utilize the advantages of nanomaterials and exploit them in red mud modification in strength aspects are rarely studied. Therefore, in this paper, nano-SiO_2 is synergistically involved in the modification of red mud-based stabilized soil, mechanical property and microstructure of the stabilized soil are experimentally studied. Based on the obtained results, the curing mechanism of nano-SiO_2 synergistically modified red mud-based stabilized soil is analyzed.

2. Materials and methods

2.1. Raw materials

2.1.1. Red mud

The red mud used in the test was taken from an aluminum company in Guangxi Province, which is a Bayer red mud. The chemical composition of the red mud is shown in Table 1. It shows that the red mud contains 5.23% of Na_2O, which can provide hydroxide for the hydration process.

Table 1. Main chemical components of red mud.

	Fe_2O_3	Al_2O_3	SiO_2	CaO	Na_2O	TiO_2	MgO	K_2O	LOL
Average value	37.08%	18.89%	12.35%	10.56%	5.23%	6.21%	0.68%	0.12%	6.23%

2.1.2. Nano-SiO_2

The nano-SiO_2 used was produced by the mechanical crushing process. The nano-SiO_2 has a large specific surface area and a high surface activity. Its technical parameters are listed in Table 2.

Table 2. Nano-SiO_2 technical parameter table.

Materials	Particle size (nm)	Purity (%)	Specific surface area (m^2 /g)	Bulk density (g/cm^3)	Color	pH
Nano-SiO_2	1~100	99.9	240	0.06	White	4-7

2.1.3. Cement

The cement used in the test is 42.5 standard ordinary silicate cement. It has a specific surface area of 340 m^2 /kg and a density of 3.10g /cm^3. The chemical composition is shown in Table 3.

Preprints (www.preprints.org) | NOT PEER-REVIEWED | Posted: 12 July 2023 doi:10.20944/preprints202307.0853.v1

Table 3. Main chemical components of cement.

Calcium oxide (CaO)	Silicon dioxide (SiO_2)	Aluminum oxide (Al_2O_3)	Iron oxide (Fe_2O_3)	Titanium dioxide (TiO_2)	Sulfur trioxide (SO_3)
65.13%	21.32%	5.35%	3.96%	0.25%	0.30%

It shows that the main mineral composition of the cement is tricalcium silicate $3CaO\text{-}SiO_2$ (C3S), accounting for 50-60%; dicalcium silicate $2CaO\text{-}SiO_2$ (C2S), accounting for 20-25%, called Belite or B ore; tricalcium aluminate $3CaO\text{-}AlO_{23}$ (C3A), accounting for 5-10%; tetra calcium iron aluminate, $4CaO\text{-}AlO_{23}\text{-}FeO_{23}$ (C4AF), accounting for 10-15%.

2.1.4. Gypsum

The selected gypsum is a kind of construction gypsum produced by Jinan Desheng Chemical Technology Co. Ltd., Shandong Province. It is white powder with a density of 2.32 g/cm^3. Its chemical formula is $CaSO_4\text{-}0.5H_2O$.

2.2. Specimen preparation

When stabilized soil is applied to the subgrade material, the strength requirements need to be met first. Combining the studies of Xue et al., (2017), Xue et al., (2016a), the designed mass ratios added in the red mud-based stabilized soil of nano-SiO_2 are 0.5%, 1%, 1.5%, 2%, 2.5% and 3%; gypsum is 6%; cement are at 1%, 3%, 5%, 7%, and 9%. Referring to Table 4.2.4 in Technical Guidelines for Construction of Highway Roadbases (JTG/T F20-2015), the 7-d unconfined compressive strength of red mud-based stabilized soil should be greater than or equal to 2 MPa, so as to serve as the base material used for medium and light traffic secondary and secondary roads.

The specimen preparation are as follows:

① Drying and grinding of red mud specimens into powder form;
② Add cement and powdered gypsum to the red mud specimen in accordance with the designed dosage and mix well;
③ Add deionized water to the specimen in accordance with the maximum dry density and optimum water content determined by the compaction test, and mix well;
④ The test material will be made into 5mm×5mm cylindrical compressive specimens, and the specimen production time should be controlled within 1 hour after adding cement;
⑤ After the specimens are made, they are left to standing curing for different periods (i.e., 1, 7, 14 and 28 days) before the mechanical and microstructure experiments.

Following the above preparation procedures, stabilized soil specimen with different contents of red mud, cement and nano-SiO_2 were prepared. The synergistic combination scheme of the added stabilizers is shown in Table 4, where NS1CS6PC3 denotes indicates that the doping mass ratio of nano-SiO_2 is 1%, the doping mass ratio of gypsum is 6%, and the doping mass ratio of cement is 3%.

Table 4. Collaborative combination scheme table.

Modified solutions	I	II	III	IV	V
PC individually modified	PC1	PC3	PC5	PC7	PC9
NS+CS6+PC3 synergistic modification	NS0.5CS6PC3	NS1CS6PC3	NS2CS6PC3	NS3CS6PC3	

 doi:10.20944/preprints202307.0853.v1

2.3. Testing methods

2.3.1. Unconfined compression test

The prepared specimens, cured for 1, 7, 14 and 28 days, respectively, were subjected to water immersion for 24 h before the unconfined compression test. The compression was conducted under the condition of the unconfined compression test is carried out using the TSZ series automatic triaxial instrument (Fig.1) produced by Nanjing Soil Instrument Factory Co. The instrument can directly obtain the experimental maximum compression strength and the relationship curve between the main stress difference and axial strain.

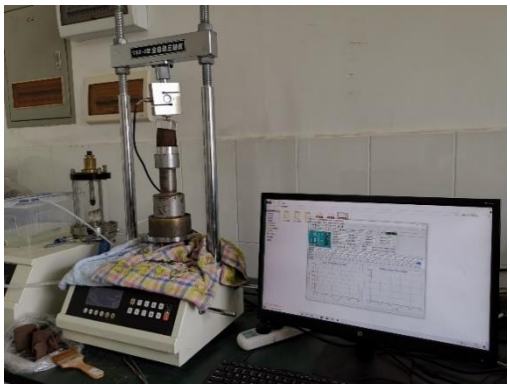

Figure 1. The TSZ series fully automatic triaxial instrument.

2.4.2. Scanning electron microscope test

A scanning electron microscope (SEM) of type S-3400 produced by Hitachi, Tokyo, Japan, was used for microstructure observation, which has a magnification of 20 ~ 30,000 times. Before observation, the dried specimen is cut into observation cubes with dimensions of 4mm (length) × 4mm (width) × 2mm (thickness) using a geotechnical knife. The natural cross-section is used as the observation surface, then the observation cube is connected to the metal panel for observation through the conductive strip, and after the specimen surface and sides are sprayed with gold, it can be tested and observed.

2.4.3. Energy spectrum analysis test

Energy spectrometry (EDX) is the analysis of all elemental species and contents between Be-U within the micro-zone of the material using an energy dispersive spectrometer, which is used in conjunction with a scanning electron microscope.

2.4.4. X-ray diffraction test

X-ray diffraction (XRD) tests are used to measure the mineral composition of test materials. Before testing, the red mud-based stabilized soil material was oven-dried, after which the samples were ground into powder form and set aside. The mineral composition was qualitatively analyzed using an X'Pert PRO MRD/XL high-resolution diffractometer. During the experiments, the ray wavelength $\lambda\kappa\alpha$ was 1.54060 Å, the tube pressure was 40 KV, the tube electric current was 40 mA, the scanning range was 5° to 75°, the step size was 0.02°, and the scanning speed was 5°/min.

2.4.5. X-ray photoelectron spectroscopy test

X-ray photoelectron spectroscopy (XPS) is an advanced analytical technique in the microscopic analysis of electronic materials and components. Before the test, the red mud-based stabilized soil material was oven-dried, after which the sample was ground into powder form and set aside. A PHI-5300ESCA X-ray photoelectron spectrometer was used for XPS analysis of the red mud-based

Preprints (www.preprints.org) | NOT PEER-REVIEWED | Posted: 12 July 2023 doi:10.20944/preprints202307.0853.v1

stabilized soil specimens with an Mg / Al anode target with 400 W power and the analyzer charge set to 17.5 eV, which was detected by a position-sensitive detector.

3. Results and analysis

3.1. The unconfined compressive strength

3.1.1. Effect of cement content

The unconfined compression tests were conducted on the cylindrical specimens of red mud-based stabilized soil mixed with cement alone at 1%, 3%, 5%, 7%, and 9%, respectively. The test results are shown in Figure 2.

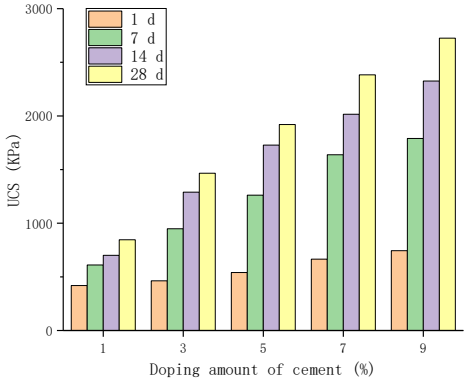

Figure 2. Effect of cement on UCS.

Cement-modified red mud-based stabilized soil has higher compressive strength with increasing cement admixture, the unconfined compressive strength of the cement-modified red mud-based stabilized soil was 491 kPa, 928 kPa, 1262 kPa, 1639 kPa, and 1797 kPa for the specimens with 1%, 3%, 5%, 7%, and 9% cement dosing, respectively.

The unconfined compressive strength of cement-modified red clay-based stabilized soil increased with the increase of curing time, but the increase of unconfined compressive strength from 1 d to 7 d was greater than the increase of curing time from 7 d to 14 d and that from 14 d to 28 d. The increase of unconfined compressive strength of cement-modified red clay-based stabilized soil was calculated as the increase of curing time from 1d to 7d and from 14 d to 28 d only. It is assumed that the presence of soluble alkali in the red mud can promote the hydration reaction, and the strength increase of the stabilized soil by the modification of cement is also mainly concentrated in the pre-curing period.

3.1.2. Effect of synergistic modification of nano-SiO_2, gypsum and cement

To verify the optimum dosing of nano-SiO_2 in the modified material, the dosing of gypsum was chosen to be 6% in this section, the dosing of cement was chosen to be 3% considering the economy, and the dosing of nano-SiO_2 was chosen to be 0.5%, 1%, 2% and 3% for the tests. Figure 3 shows the relationship between the unconfined compressive strength of the modified material and the variation of nano-SiO_2 dosing. It can be found that the unconfined compressive strength did not increase with the increase of nano-SiO_2 dosing, and the unconfined compressive strength was maximum at 1% dosing. For example, the unconfined compressive strength at 7 d curing time is 2421, 2748, 2467 and 2156 kPa for 0.5%, 1%, 2%, and 3% of nano-SiO_2, respectively. They all satisfy the condition of 7 d unconfined compressive strength of red mud-based stabilized soil as proposed in Section 2.2.

Preprints (www.preprints.org) | NOT PEER-REVIEWED | Posted: 12 July 2023 doi:10.20944/preprints202307.0853.v1

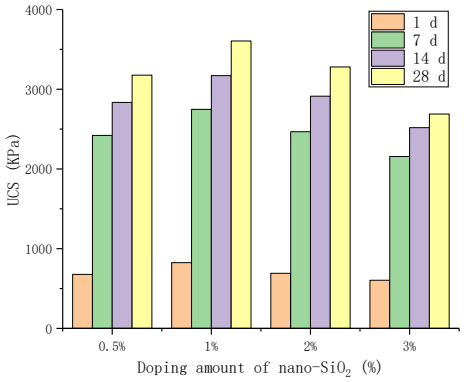

Figure 3. Effect of nano-SiO_2 content on UCS of gypsum and cement synergistic combination.

Figures 3 show that the unconfined compressive strength of the modified red mud-based stabilized soil increased with the increase of the maintenance time, and the growth rate of the unconfined compressive strength was the largest from 1 to 7 d in the early stage. In the case of 1% dosing of nano-SiO_2, The growth value of the first 7d compressive strength accounted for 69.2% of the growth value of the 28d compressive strength. The highest unconfined compressive strength of the modified combination can be obtained at 1% of nano-SiO_2. Wang et al. (2020) concluded that when the nano-SiO_2 doping is too much, the nano-SiO_2 tends to form agglomerates and adsorb water, encroaching on the water for hydration reaction, affecting the degree of hydration and causing the strength of the red mud-based stabilized soil to decrease, so the NS2CS6PC3 and NS3CS6PC3 combinations have lower unconfined compressive strengths than the NS1CS6PC3 combination.

Figure 4 shows that the age of 7d was the inflection point of unconfined compressive strength growth rate, and after 7d the growth rate of unconfined compressive strength gradually decreases after the age of 7d, and the average growth rate of unconfined compressive strength is 7.4 kPa/d during 60d~120d.

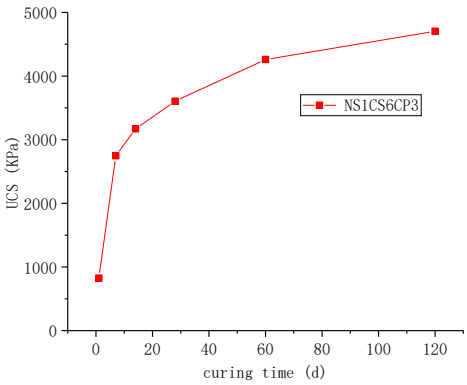

Figure 4. Curve of UCS of NS1CS6PC3 combination with curing time.

3.2. Micro-morphology and curing characteristics of red mud-based stabilized soil

3.2.1. Micromorphology

The gypsum dose of 6%, the cement dose of 3%, and the nano-SiO_2 dose of 1%, 2%, and 3%, respectively, were selected for electron microscope scanning at 28 d. The observation magnification of the electron microscope used in the test was 500 times. The SEM images after the test are shown in Figure 5. It shows that the structural compactness of the soil did not increase with the increase of nano-SiO_2 under the condition of a certain amount of gypsum and cement admixture. On the contrary, it showed a decreasing trend, which indicates that in the synergistic modification combination of nano-SiO_2, gypsum and cement, there exists a limit for the amount of nano-SiO_2. When the admixture of nano-SiO_2 is 1%, the surface of the soil is relatively flat, the pore development is less, the fracture rate is low, and the soil structural compactness is relatively good.

Preprints (www.preprints.org) | NOT PEER-REVIEWED | Posted: 12 July 2023 doi:10.20944/preprints202307.0853.v1

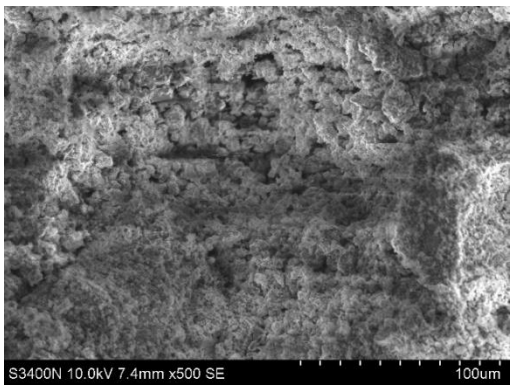

(a) SiO nanoparticles$_2$ at 1%, gypsum at 6%, cement at 3%

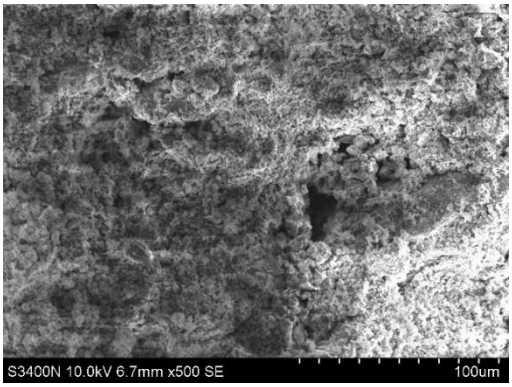

(b) SiO nanoparticles$_2$ at 2%, gypsum at 6%, and cement at 3%

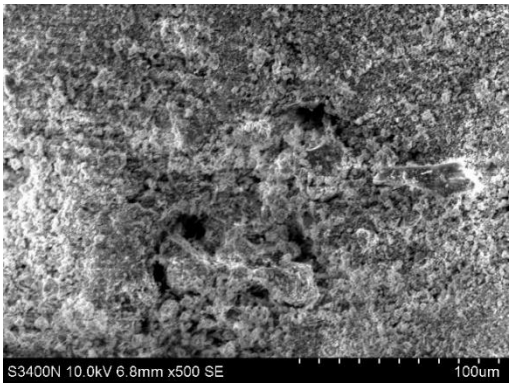

(c) SiO nanoparticles$_2$ at 3%, gypsum at 6%, cement at 3%

Figure 5. 500 times SEM images of red mud stabilized soil modified by nano-SiO_2, gypsum, and cement.

3.3.2. Curing characteristics

(1) SEM-EDX

The gypsum dose of 6%, the cement dose of 3%, and the nano-SiO_2 dose of 1%, 2%, and 3%, respectively, were selected for electron microscope scanning at 28 d. The observation magnification of the electron microscope used in the test was 10,000 times. The SEM images after the test are shown in Figure 6.

The content and morphology of some gelling products in the 10,000x electron microscope scan images differ. Figure 6(a), the gelling products are mainly needle-like and columnar calcium alumina (AFt), and the AFt is longitudinally and horizontally distributed between particles or agglomerates, interconnected and interwoven, forming a huge spatial mesh structure to support the material skeleton system, while $Ca(OH)_2$ is occasionally seen to be distributed; Figure 6(b), the gelling products are mainly columnar AFt, which is in clusters Figure 6(c), the gelling products are not obvious, and the distribution of needle-like AFt is occasionally seen, and the red mud agglomerates are also found. It is assumed that the excessive nano-SiO_2 fills and blocks the pores and channels of the stabilized soil, which reduces the migration of ions such as OH^-, Ca^{2+}, and Al^{3+}, and hinders the generation of AFt and other products.

The synergistic participation of gypsum promotes more AFt generation, which is more obvious at nano-SiO_2, doping of 1% and 2%. AFt is generated by the reaction between gypsum and tricalcium aluminate in cement clinker with the reaction equation: $3C3A+3(CaSO_4 \cdot 2H_2O)+26H_2O \rightarrow 3CaO \cdot Al_2O_3 \cdot 3CaSO_4 \cdot 32H_2O$. Usually The percentage of gypsum in silicate cement is less than 3%, while 6% of gypsum is added to this group of modified materials, which makes the red mud-based stabilized soil materials have the conditions to generate more AFt.

Preprints (www.preprints.org) | NOT PEER-REVIEWED | Posted: 12 July 2023 doi:10.20944/preprints202307.0853.v1

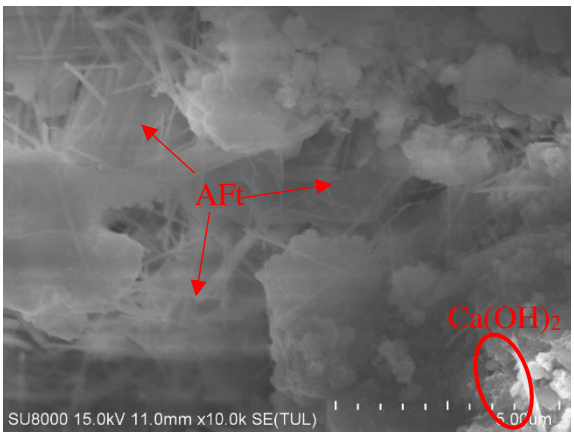

(a) SiO nanoparticles$_2$ at 1%, gypsum at 6%, cement at 3%

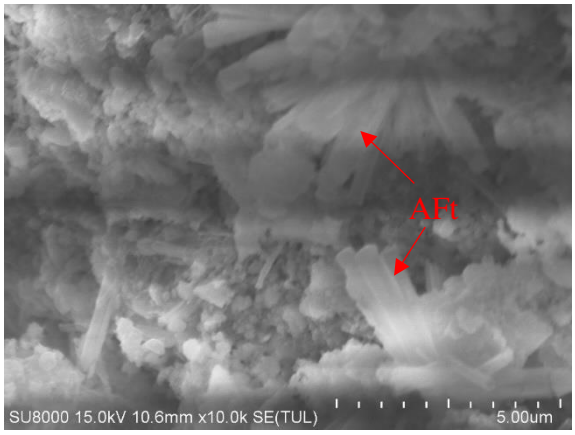

(b) NS at 2%, CS at 6%, PC at 3%

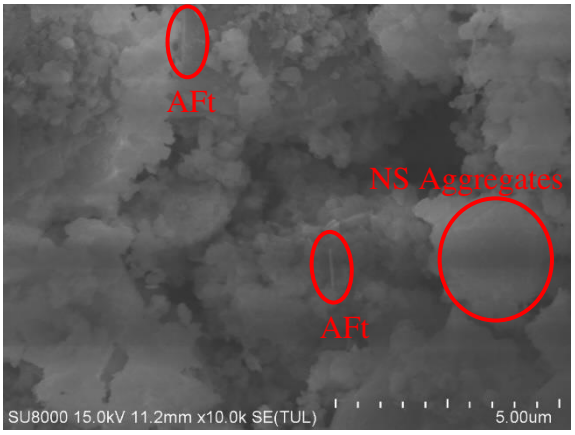

(c) NS at 3%, CS at 6%, PC at 5%

Figure 6. 10000 times SEM images of red mud stabilized soil modified by nano-SiO_2, gypsum, and cement.

Figure 7 shows the EDX energy spectrum of the NS1CS6PC3 modified combined agglomerates. Compared with the EDX energy spectrum of pure red mud, the presence of S elements within the stabilized soil material indicates that gypsum intervenes in the reaction and the material has a higher content of O and Ca elements, presumably more AFt is generated within the modified material.

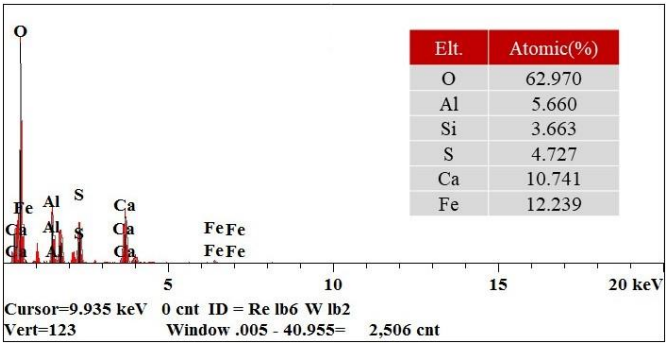

Elt.	Atomic(%)
O	62.970
Al	5.660
Si	3.663
S	4.727
Ca	10.741
Fe	12.239

Figure 7. EDX energy spectrum of NS1CS6PC3 modified composite aggregate.

(2) XRD

Figure 8 shows that the XRD pattern of modified red mud-based stabilized soil is similar to that of red mud in terms of peak area, peak size, and peak trend, mainly because the amount of modified materials in red mud-based stabilized soil is very small, and the new material generation should be

Preprints (www.preprints.org) | NOT PEER-REVIEWED | Posted: 12 July 2023 doi:10.20944/preprints202307.0853.v1

relatively limited. However, due to the addition of the modified materials, new products were generated, so its XRD pattern had peaks that were not present in the red mud XRD pattern.

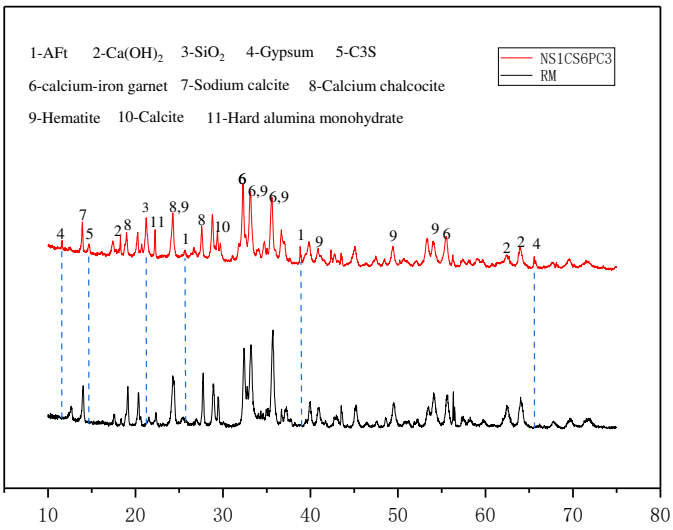

Figure 8. XRD patterns of NS1CS6PC3 modified red mud stabilized soil and red mud.

The XRD pattern of the modified red mud-based stabilized soil contains physical phases of hematite, calcium-iron garnet, sodium calcite, calcium chalcocite, and calcite in red mud, and also contains physical phases of AFt, silica, gypsum, and tricalcium silicate, which are not present in red mud, where AFt is a hydration product, tricalcium, gypsum and silica are incompletely reacted modified materials. The peak of $Ca(OH)_2$ in the modified red mud spectrum overlaps with the red mud, and the analysis of this peak may be the physical phase of portlandite in the red mud (Rao, 2008), and the main peak does not see the hydrated Ca(OH)2 physical phase. According to the analysis, after the hydration reaction between the cement with little admixture and the water contact in the modified material, the hydrated $Ca(OH)_2$ is generated, but the alumina and silicon oxide, which exist in large quantities in the red mud, react with the hydrated Ca(OH)2 of cement under the alkaline environment conditions in a pozzolanic reaction, and the $Ca(OH)_2$ generated by its hydration is also small due to the little admixture of the cement, then the alumina and silicon oxide, which exist in large quantities in the red mud, gradually consume the hydrated $Ca(OH)_2$. The cement hydration products, C-S-H gels, and C-A-H gels, have no peaks in the XRD patterns because of their non-crystalline structure.

(3) XPS

The binding energy refers to the mutual attraction between the components within an object that binds them together, and if one wants to separate these components, a certain amount of energy is required to overcome the attraction between them, which is the binding energy of the object, and the amount of work required indicates the tightness of the combination of these components. The greater the binding energy, the greater the attraction or cohesion between the components of the material (Zhang et al., 2009).

Based on the XPS energy spectra of the red mud-based stabilized soil materials with different modification combinations and different hydration ages, the binding energies of the main elements such as Ca, Si, Al, Na, O, and S during hydration can be derived, as shown in Table 5.

Table 5. Binding energy table of main elements of different modified samples at different curing ages.

Modified specimens	Conservation age/d	Binding energy/eV					
		Ca2p	Si2p	Al2p	Na1s	O1s	S2p
NS1CS6PC3	7	346.90	102.17	74.14	1071.71	531.32	169.09

	28	346.97	102.18	74.18	1071.76	531.33	169.28
	60	347.05	102.23	74.23	1071.94	531.44	169.61
NS2CS6PC3	60	347.04	102.47	74.22	1071.72	531.47	169.55
NS3CS6PC3	60	346.96	102.65	74.32	1071.63	531.58	169.50

As shown in Table 4, in the same set of modified materials, the binding energy of the main elements such as Ca, Si, Al, Na, O, and S in the red mud-based stabilized soil materials are increasing with the increase of the maintenance age, which indicates that the free Ca, Si, Al, Na, O and S elements in the liquid phase of the red mud-based stabilized soil materials continuously participate in the hydration reaction with the increase of the maintenance age and generate $Ca(OH)_2$, C-S-H gels, AFt and other hydration products, while new covalent and ionic bonds are formed in this process, which makes the binding energy of each element enhanced (Zhang et al., 2014).

However, the increase or decrease of the binding energy of each major element with different doping amounts of nano-SiO_2 did not exactly show a positive or negative correlation with the amount of nano-SiO_2. It is speculated that this phenomenon is related to the elemental properties and the calcium-silicon ratio.

4. Curing Mechanics of red mud-based stabilized soil

We analyze the properties and change mechanisms of red mud-based stabilized soils by SEM-EDX, MIP, XRD, and XPS, and conclude that the curing mechanisms of red mud-based stabilized soils include hydration reactions, pozzolanic reactions (secondary hydration reactions), the promotion effect of nano-SiO_2 and the enhancement effect of gypsum, which are chemical reactions. In the case of stabilized soil bulk materials, the premise for these reactions is that the materials first undergo a physical process - mechanical compaction - and when mechanically compacted, the bulk materials are tightly joined together so that they have the contact conditions for chemical reactions to occur between them. The curing mechanisms are independent of each other but are interconnected and the common interconnection formed a synergistic curing mechanism that promotes the formation of the strength of the red mud-based stabilized soil.

4.1. Mechanical compaction

Through mechanical compaction, the friction and embedded force between the particles of the red mud-based stabilized soil material formed, and the friction and embedded force between the particles contributed to the macroscopic mechanical strength, which is the mechanism of mechanical compaction to obtain the strength of the material. Once the particles of the red mud-based stabilized soil material are in close contact with each other through mechanical compaction and have gained initial strength, the chemical reaction between the mixes continues to occur as the maintenance time increases, generating cementing substances that result in tighter particle bonding and higher structural strength.

4.2. Hydration reaction and volcanic ash reaction

The modified material in the red mud-based stabilized soil contains cement clinker, which is highly reactive. When it meets water, each component of the cement dissolves rapidly and undergoes a hydration reaction, which is the main reason for the strength of red mud-based stabilized soil. The hydration reaction of cement is a series of reactions of tricalcium silicate (C3S), dicalcium silicate (C2S), tricalcium aluminate (C3A), and tetra calcium iron aluminate (C4AF) in cement with the participation of water, and the process of hardening strength of the material is improved by the generation of cementitious products.

Pozzolanic reaction, also known as secondary hydration reaction, refers to the process that active components such as SiO_2, and Al_2O_3 in minerals react with $Ca(OH)_2$ in an alkaline environment to produce gelling products such as C-S-H, C-A-H, AFt, etc. (Peng, 2020).The proportion of SiO_2, and Al_2O_3 in red mud is 12.35% and 18.89% respectively, and the active component accounts for a

 doi:10.20944/preprints202307.0853.v1

relatively large proportion; nano SiO_2 soluble in alkali, in the alkaline environment belongs to the active material, can provide Si^{4+}; gypsum can provide additional Ca^{2+}; red mud soluble alkali such as NaOH, KOH and can provide OH^- in addition to cement hydration and then supplement OH^-. Therefore, the modified red mud-based stabilized soil itself already has good conditions for the pozzolanic reaction. The pozzolanic reaction is an important reason for the late strength growth of red mud-based stabilized soil.

4.3. Facilitating effect of nano-SiO_2

The synergistic participation of nano-SiO_2 improves the strength of the red mud-based stabilized soil. The contribution of nano-SiO_2 is reflected in the promotion of the early hydration process and hydration degree through the "nucleation effect" on the one hand, the provision of more active silicon sources on the other hand, and the generation of more cementation products under alkaline environment on the other hand, and the reduction of material porosity and improvement of material compactness through the filling effect.

4.3.1. Promotion of early hydration reaction

According to Jianrong Wang (2019), G. Land et al. (2012), the high specific surface area of nano-silica and its high activity in the alkaline environment make it have a "crystalline nucleation effect", and the nano-silica uniformly distributed in the red mud-based stabilized soil acts as The nano-silica uniformly distributed in the red mud-based stabilized soil acts as a "nucleation crystal species", providing nucleation sites, allowing more hydration ions to gather and react in the periphery, accelerating the early hydration process of the red mud-based stabilized soil, promoting the early production of more hydration products, and improving the strength of the red mud-based stabilized soil.

For the characteristics of the granular material of the red mud-based stabilized soil, the model of nano-SiO_2 promoting the early hydration process of the red mud-based stabilized soil was established in this study with individual red mud particles, see Figure 3-9.

In the first step, as shown in Figure 3-9(a), the ground red mud in powder form is mixed with the modified material in a dry state so that the material particles are uniformly distributed. The red mud particles are surrounded by the cement, while the smaller particle size nano-SiO_2 is filled between the red mud and cement particles.

In the second step, as shown in Figure 3-9(b), water is added to the mixed particles in the designed proportion, and the hydration reaction occurs rapidly after the water is added, and the hydration products are formed around the cement particles, while the "nucleation effect" formed by the nano-SiO_2 due to its high surface energy makes the hydration ions of cement also gather around it rapidly, which in turn makes the hydration products are also formed around it and gathered around it.

In the third step, as shown in Figure 3-9(c), with the hydration reaction, the hydration products are continuously generated. The original state of large pores between cement particles due to the small amount of cement and the hydration products are not easily connected in series, due to the dispersed presence of nano-SiO_2 and the continuous gathering of hydration products around themselves, the cement particles can be continuously connected and bonded by nano-SiO_2 and hydration products.

Preprints (www.preprints.org) | NOT PEER-REVIEWED | Posted: 12 July 2023 doi:10.20944/preprints202307.0853.v1

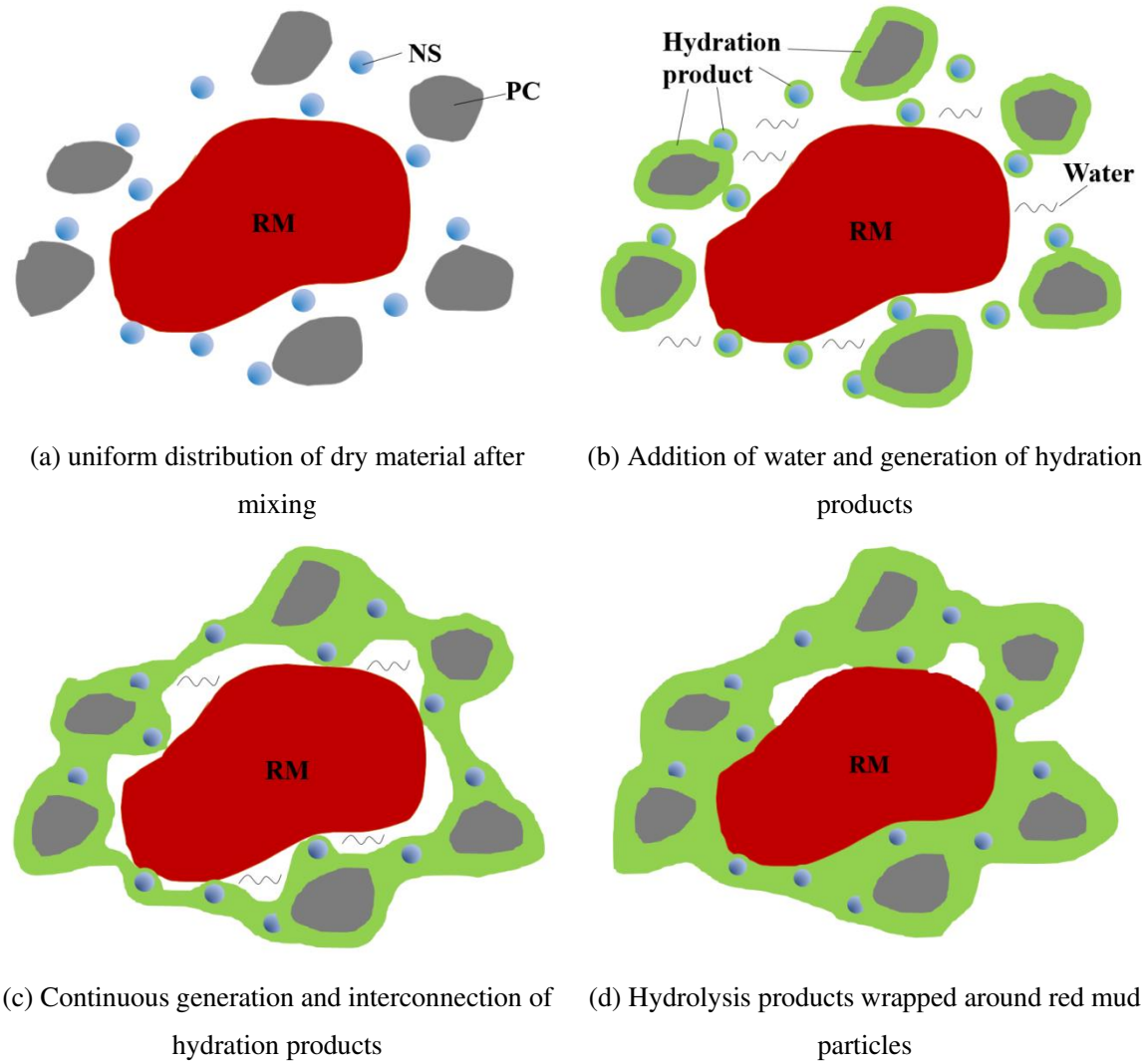

(a) uniform distribution of dry material after mixing

(b) Addition of water and generation of hydration products

(c) Continuous generation and interconnection of hydration products

(d) Hydrolysis products wrapped around red mud particles

Figure 3-9. Model diagram of nano-SiO_2 synergistic promoting hydration process.

In the fourth step, as shown in Figure 3-9(d), the hydration reaction continues and the hydration products keep connecting to fill the particle voids, and finally a network body is formed around the red mud particles, which wraps the red mud particles and also serves to bond the different red mud particles, thus improving the overall compactness and structural strength of the red mud-based stabilized soil. The variation of this step can be better explained by the staggered distribution of Aft and wrapping of red mud particles shown in Figure 3-6(a).

The content of C3S is about 50-60% in cement, which is the main contributor to the early strength of cement, then the promotion effect of nano-SiO_2 is mainly concentrated in the early stage during the synergistic process of nano-SiO_2, which is the mechanism of nano-SiO_2 to promote the early hydration reaction.

4.3.2. Provide silicon source

Nano-silica is stable but soluble and reactive under alkaline environmental conditions, so the synergistic participation of nano-SiO_2 continuously replenishes the liquid-phase system with Si^{4+} ions, providing more silicon sources for the red mud-based stabilized soil. Si^{4+} provided by nano-SiO_2 and Ca^{2+} together with OH^- ions (generated by cement hydration and by soluble alkali in red mud) in turn undergo secondary hydration reactions to generate more C-S-H, C-A-H, AFt and other gels, further enhancing strength. The red mud acts as a "hotbed", and the alkali environment provided by

Preprints (www.preprints.org) | NOT PEER-REVIEWED | Posted: 12 July 2023 doi:10.20944/preprints202307.0853.v1

it allows the relatively stable nano-SiO_2 and gypsum to react continuously, but the reaction is more moderate and can last for a longer period.

4.4. Enhancement effect of gypsum

The synergistic involvement of CS in the modified material likewise significantly improved the mechanical strength of the red mud-based stabilized soil. The gypsum was blended at 6%, and in an alkaline environment, gypsum was gradually dissolved in the liquid phase, which could continuously provide Ca^{2+} ions to the liquid phase system. During the hydration of cement, tricalcium aluminate C3A reacts with $Ca(OH)_2$ and gypsum to form trisulfate hydrated calcium sulfate (AFt), and simply in the cement system, if gypsum is insufficient and consumed before C3A is fully hydrated, the trisulfate hydrated calcium sulfate will again react with the unconsumed C3A to convert into monosulfate hydrated calcium sulfate (AFm). According to Wenwen Tian (2020), Shuhua L (2010), and others, the strength of AFt or its contribution to material strength is greater than that of AFm, so once AFt is converted to AFm, it will have a negative impact on material strength. Since the red mud-based stabilized soil modification material has an additional 6% gypsum co-added in addition to 3% cement, the amount of gypsum is sufficient for the hydration reaction, and it is presumed that all or the vast majority of the end product of C3A in cement is AFt, which enhances the strength of the modified stabilized soil. Figure 3-6 shows the characteristics.

4.5. Effect of calcium to silicon ratio

In the alkaline environment of red mud, the modified material and the active ingredients in red mud are excited and chemically reacted to produce more cementation products and promote strength. Different materials have different calcium-silica ratios, and different calcium-silica ratios have different effects on material strength.

Calculation of calcium to silicon ratio based on Equation 1:

$$\frac{C}{S} = \frac{CaO\ total\ content \div 56}{SiO_2\ total\ content \div 60} \quad (1)$$

Where, the total calcium oxide content = ∑ material ratio × calcium oxide content, the total silicon oxide content = ∑ material ratio × silicon oxide content.

The calculated calcium-silica ratios of NS1CS6PC3, NS2CS6PC3, and NS3CS6PC3 were 2.83, 2.55, and 2.32, respectively, which were higher than 0.92 for red mud and lower than 3.23 for cement, and the addition of modified materials improved the calcium-silica ratio of red mud and the calcium-silica ratio was close to that of cement. section 3.1.2 revealed that the unconfined compressive strengths of NS1CS6PC3, NS2CS6PC3, and NS3CS6PC3 at the age of 7 d were 2748, 2467 and 2156 kPa, respectively, indicating that the unconfined compressive strength increased with the increase in calcium-silica ratio in the three groups of modified materials. It indicates that the increase of calcium-silica ratio in the tested red mud-based stabilized soil contributes to the improvement of the strength of the red mud-based stabilized soil.

5. Conclusions

In this experiment, the stabilized soil material was prepared by modifying the red mud of aluminum industrial waste, and the strength and microscopic characteristics of the red mud-based stabilized soil with different modified materials and different amounts of modified materials were tested, and the curing mechanism was analyzed, and the main findings were as follows:

(1) Cement alone can improve the unconfined compressive strength of red mud-based stabilized soil; with the synergistic modification of nano-SiO2, gypsum and cement, the 7-d unconfined compressive strength of red mud-based stabilized soil is greater than 2 MPa under the synergistic effect of nano-SiO2 (1%, 2% and 3%, respectively), which meets the compressive strength requirement of road subgrade material, and the highest unconfined compressive strength of nano-SiO2 combination is 2748 kPa.

(2) In the microstructure study, the SEM test results showed that the soil structural compactness did not increase with the increase of nano-SiO_2 when nano-SiO_2, gypsum, and cement were co-modified, and the soil structural crack rate was the lowest and the structural compactness was the best when nano-SiO_2 was used at 1%.

(3) High magnification SEM tests reveal that when nano-SiO2, gypsum and cement are synergistically modified, it is found that the increase of needle-like and columnar AFt in the cementitious products is due to the 6% gypsum added to the modified material, which creates conditions for the formation of more AFt; The XRD results showed that the gypsum diffraction peaks of the NS1CS6PC3 modified combination of red clay-based stabilized soil tended to disappear with the growth of the maintenance age, indicating that it was continuously transformed into AFt. The increase of binding energy of hydration product-related ions in the modified material also indicates the strength of the modified material is improved.

(4) Mechanical compaction is a prerequisite for chemical curing, and the chemical curing mechanism contains the hydration reaction, pozzolanic reaction, the promotion effect of nano-SiO2, and the enhancement effect of gypsum. The amount of nano-SiO_2 is small, but it can promote the early hydration reaction process and hydration degree, provide more silica source for the stabilized soil material; The paper established a model of nano-SiO_2 to promote the early hydration process of red clay-based stabilized soil, and revealed the mechanism of nano-SiO_2 to promote the hydration process of red clay-based stabilized soil; the modification effect of gypsum is key in providing a calcium source to the red clay-based stabilized soil system The key role of gypsum in the modification is to provide a calcium source, which contributes to the conversion of all or most of the C3A in cement into AFt, and at the same time, with Si^{4+} ions in the material, to generate C-S-H hydration gel under alkaline environment, which further enhances the strength of the modified stabilized soil.

References

1. Adamu M, Mohammed B S, Shafiq N, et al. Skid Resistance of nano silica modified roller compacted rubbercrete for pavement applications: Experimental methods and response surface methodology [J]. Cogent Engineering, 2018, 5(1) 1452664.
2. Almurshedi A D, Thijeel J K, Al-Awad K. Mitigation of collapse of marshes soil by nano silica fume [J]. IOP Conference Series: Materials Science and Engineering, 2020, 737:012110.
3. Atan E, Sutcu M, Cam A S. Combined effects of bayer process bauxite waste (red mud) and agricultural waste on technological properties of fired clay bricks [J]. Journal of Building Engineering, 2021, 43(3):103194.
4. Elżbieta Bombik and Antoni Bombik and Katarzyna Rymuza. "The influence of environmental pollution with fluorine compounds on the level of fluoride in soil, feed and eggs of laying hens in Central Pomerania, Poland". Environmental Monitoring and Assessment: An International Journal Devoted to Progress in the Use of Monitoring Data in Assessing Environmental Risks to Man and the Environment 192.4(2020): 319-324.
5. Farajzadehha S, Mahdikhani M, Moayed R Z, et al. Experimental study of permeability and elastic modulus of plastic concrete containing nano silica[J]. Structural Concrete, 2022, 23(1):521–532.
6. GB/T9776-2022, Calcined gypsum [S]. Beijing: China Standard Publishing House, 2022.
7. G.Land, D.Stephan The influence of nano-silica on the hydration of ordinary Porland cement [J]. Journey of material science. 2012(47):1011-1017.
8. JTG/T F20-2015, Technical Guidelines for Construction of Highway Roadbases [S]. Beijing:Ministry of Transport of the People's Republic of China, 2015.
9. Kulkarni P P, Mandal J N. Strength evaluation of soil stabilized with nano silica- cement mixes as road construction material [J]. Construction and Building Materials, 2022, 314:125363.
10. Liang X, Ji Y. Mechanical properties and permeability of red mud-blast furnace slag-based geopolymer concrete [J].SN Applied Sciences, 2021, 3(1): 1-10.
11. Liu S T, Li Z Z, Li Y Y, et al. Strength properties of Bayer red mud stabilized by lime-fly ash using orthogonal experiments [J]. Construction & Building Materials, 2018, 166(30):554-563.
12. Li S, Zhang J, Li Z, et al. Feasibility study on grouting material prepared from red mud and metallurgical wastewater based on synergistic theory [J]. Journal of Hazardous Materials, 2020, 407(5):124358.
13. Li Z F, Gao Y F, Zhang M, et al. The enhancement effect of Ca-bentonite on the working performance of red mud-slag based geopolymeric grout [J]. Materials Chemistry and Physics, 2022, Volume 276(35): 125311.

14. Li K, Wei Z Q, Qiao H X, et al. Experimental study on the performance of nano-SiO2 modified polymer cementitious materials[J]. Journal of Hunan University: Natural Science Edition, 2021, 48(11):10. (in Chinese)
15. Liu S H, Yan P Y. Effect of Limestone Powder on Microstructure of Concrete [J]. Journal of Wuhan University of Technology: Materials Science English Edition, 2010(2):4.
16. Mukiza E, Zhang L L, Liu X, et al. Utilization of red mud in road base and subgrade materials: A review[J]. Resources, Conservation and Recycling, 2019, 141: 187-199.
17. Ou X D, Chen S J, Jiang J, et al. Reuse of Red Mud and Bauxite Tailings Mud as Subgrade Materials from the Perspective of Mechanical Properties [J]. Materials, 2022, 15(3):1123.
18. Peng, Y S. Multi-scale properties of bauxite tailings foam lightweight soils and their variation mechanisms [D]. Nanning:Guangxi University, 2020.
19. Rao, P P. Study on the stability of Pingguo Aluminum Flatland-type red mud tailing dam in Guangxi[D]. Nanning:Guangxi University, 2008.
20. Suo C, Wen H, Cao J, et al. Performance of a Composite Soil Prepared with Red Mud and Desulfurized Gypsum [J]. KSCE Journal of Civil Engineering, 2022, 26:47-51.
21. Tian W W, Wang Q, Zhang Y, et al. Study on the performance of phosphogypsum-doped sulfo-aluminate cement for concrete canvas [J]. Journal of Three Gorges University (Natural Science Edition), 2020, 42(06):56-60. (in Chinese)
22. Wang S, Jin H, Deng Y, et al. Comprehensive utilization status of red mud in China: A critical review [J]. Journal of Cleaner Production, 2020, 289(11):125136.
23. Wang Y G, Geng Y F, Zhang H M, et al. Effect of nano-silica on alkaline slag cement flooding[J]. Silicate Bulletin, 2020, 39(05):1451-1456+1465. (in Chinese)
24. Wang J B, Du P, Zhou H Z, et al. Effect of nano-silica on hydration, microstructure of alkali-activated slag [J]. Construction and Building Materials, 2019, 220(30):110-118.
25. Xue S G，Kong X F，Zhu F，et al． 2016a． Proposal for management and alkalinity transformation of bauxite residue in China [J]．Environmental Science and Pollution Research， 23 (13) : 12822-12834
26. Xie W , Zhou F , Liu J ,et al. Synergistic reutilization of red mud and spent pot lining for recovering valuable components and stabilizing harmful element [J].Journal of Cleaner Production, 2020, 243(Jan.10):118624.1-118624.12.
27. Xue S.G., Li X.F., Kong X.F., et al. Advances in alkalinity regulation of red mud[J]. Journal of Environmental Science, 2017, 37(08):2815-2828. (in Chinese)
28. Zhu F，Li Y B，Xue S G，et al． 2016a． Effects of iron-aluminium oxides and organic carbon on aggregate stability of bauxite residues [J]．Environmental Science and Pollution Research，23 (9) : 9073-9081
29. Zhang J, Li C. Experimental Study on Lime and Fly Ash–Stabilized Sintered Red Mud in Road Base [J]. Journal of Testing and Evaluation, 2018, 46(4):36-45.
30. Zhang Y, Liu X, Xu Y, et al. Synergic effects of electrolytic manganese residue-red mud-carbide slag on the road base strength and durability properties [J]. Constrction and Building Materianls, 2019, 220: 364-374.
31. Zhang H Q. Encyclopedia of China [M]. Beijing: Encyclopedia of China Publishing House, 2009.
32. Zhang N, Liu X M, Sun H H. XPS analysis of the hydration process of red mud-gangue-based cementitious materials [J]. Metal Mining, 2014(03):171-176 (in Chinese)